NEURAL REGENERATION RESEARCH
Volume 8, Issue 11, April 2013

www.nrronline.org

doi:10.3969/j.issn.1673-5374.2013.11.006 [http://www.nrronline.org; http://www.sjzsyj.org]
Wang FY, Xu BN, Sun ZH, Wu C, Zhang XJ. Wall shear stress in intracranial aneurysms and adjacent arteries. Neural Regen Res. 2013;8(11):1007-1015.

Wall shear stress in intracranial aneurysms and adjacent arteries☆

Fuyu Wang[1], Bainan Xu[1], Zhenghui Sun[1], Chen Wu[1], Xiaojun Zhang[2]

1 *Department of Neurosurgery, Chinese PLA General Hospital, Beijing 100853, China*
2 *College of Mechanical Engineering and Applied Electronics Technology, Beijing University of Technology, Beijing 100124, China*

Abstract

Hemodynamic parameters play an important role in aneurysm formation and growth. However, it is difficult to directly observe a rapidly growing *de novo* aneurysm in a patient. To investigate possible associations between hemodynamic parameters and the formation and growth of intracranial aneurysms, the present study constructed a computational model of a case with an internal carotid artery aneurysm and an anterior communicating artery aneurysm, based on the CT angiography findings of a patient. To simulate the formation of the anterior communicating artery aneurysm and the growth of the internal carotid artery aneurysm, we then constructed a model that virtually removed the anterior communicating artery aneurysm, and a further two models that also progressively decreased the size of the internal carotid artery aneurysm. Computational simulations of the fluid dynamics of the four models were performed under pulsatile flow conditions, and wall shear stress was compared among the different models. In the three aneurysm growth models, increasing size of the aneurysm was associated with an increased area of low wall shear stress, a significant decrease in wall shear stress at the dome of the aneurysm, and a significant change in the wall shear stress of the parent artery. The wall shear stress of the anterior communicating artery remained low, and was significantly lower than the wall shear stress at the bifurcation of the internal carotid artery or the bifurcation of the middle cerebral artery. After formation of the anterior communicating artery aneurysm, the wall shear stress at the dome of the internal carotid artery aneurysm increased significantly, and the wall shear stress in the upstream arteries also changed significantly. These findings indicate that low wall shear stress may be associated with the initiation and growth of aneurysms, and that aneurysm formation and growth may influence hemodynamic parameters in the local and adjacent arteries.

Fuyu Wang☆, M.D., Attending physician.

Corresponding author: Bainan Xu, M.D., Ph.D., Chief physician, Department of Neurosurgery, Chinese PLA General Hospital, Beijing 100853, China, shjwkk@sina.com.

Received: 2012-12-21
Accepted: 2013-03-07
(N20120601002)

Key Words

neural regeneration; wall shear stress; hemodynamic parameters; intracranial aneurysm; fluid-solid coupled model; growth; formation; CT angiography; second reconstruction; multiple aneurysms; numerical simulation; grants-supported paper; neuroregeneration

Research Highlights

(1) This study reconstructed aneurysm models prior to and after aneurysm formation and growth, to investigate possible associations between hemodynamic parameters and the initiation and growth of intracranial aneurysms.
(2) Low wall shear stress may be associated with the initiation and growth of aneurysms. With increasing size of the aneurysm, the area of low wall shear stress increased, and the wall shear stress at the dome of the aneurysm decreased significantly. Aneurysm formation and growth may influence the hemodynamic parameters in local and adjacent arteries.

INTRODUCTION

Rupture of an intracranial aneurysm may cause subarachnoid hemorrhage, resulting in substantial morbidity and mortality. Local hemodynamic parameters are believed to play an important role in aneurysm growth and rupture[1]. Wall shear stress is a flow-induced stress that can be described as the frictional force of viscous blood, which may act on endothelial cell function and gene expression as well as on cell shape and structure. There is increasing evidence that wall shear stress plays a role in the evolution of aneurysmal disease[2]. Geometry has a very important influence on the hemodynamic parameters within aneurysms, and is one of the most important factors used to predict growth and rupture of aneurysms[3]. As an aneurysm grows, the hemodynamic parameters within the aneurysm may change because of the enlarged cavity[4-5]. However, it is not clear whether blood flow in the parent artery and adjacent vessels is affected, or whether formation of new aneurysms can influence hemodynamic parameters within existing aneurysms. It is therefore very important to elucidate the relationships between hemodynamic parameters and changes in aneurysm morphology, and to identify changes in flow dynamics at the different stages of aneurysm progression. However, as most aneurysms are treated once they have been diagnosed, it is difficult to study hemodynamic changes resulting from aneurysm growth, or to directly observe the rapid development of a *de novo* aneurysm. Some researchers have tried to assess hemodynamic parameters after virtual removal of the aneurysm and reconstruction of the parent artery[6].

In this study, we used CT angiography data to construct a model of a patient with an internal carotid artery aneurysm and an anterior communicating artery aneurysm. We then constructed further models by removing the aneurysm and an anterior communicating artery aneurysm and progressively decreasing the size of the internal carotid artery aneurysm to simulate the pre-formation and growth stages of the aneurysms. The models were analyzed to examine the relationships between changes in the geometric morphology of the internal carotid artery aneurysm and the hemodynamic parameters within the aneurysm and in the adjacent blood vessels, and to compare the hemodynamic parameters before and after the formation of the aneurysm and an anterior communicating artery aneurysm, to identify the hemodynamic changes during different stages of aneurysm progression, and any possible contribution of the hemodynamic parameters to the process of aneurysm progression.

RESULTS

Construction of aneurysm models in different stages of aneurysm formation

Using MIMICS 10.0 software (Belgium Materialise Company, Leuven, Belgium), we defined the region of interest and extracted the luminal surface from the three-dimensional raster gray-scale image to construct the post-aneurysm and an anterior communicating artery aneurysm formation model. We then constructed a pre-aneurysm and an anterior communicating artery aneurysm formation model by removing the aneurysm and an anterior communicating artery aneurysm, and further adjusted this model to construct a pre-internal carotid artery aneurysm growth model-2 (by decreasing the size of the internal carotid artery aneurysm) and a pre-internal carotid artery aneurysm growth model-1 (by further decreasing the size of the internal carotid artery aneurysm; Figure 1).

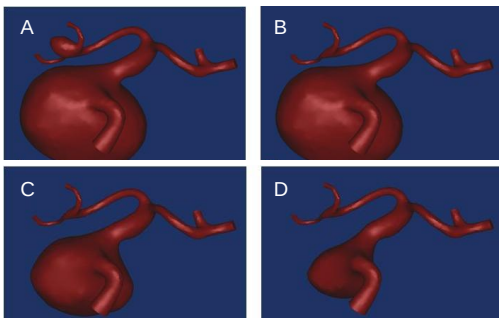

Figure 1 CT angiography of the models of the stages of aneurysm formation and growth.

(A) Post-anterior communicating artery (ACoA) aneurysm formation. (B) Pre-ACoA aneurysm formation: the ACoA aneurysm was removed. (C) Pre-internal carotid artery (ICA) aneurysm growth model-2: the ICA aneurysm was decreased in size. (D) Pre-ICA aneurysm growth model-1: the ICA aneurysm was further decreased in size.

The volume of the post-ACoA aneurysm formation model was 7 608 mm^3, the volume of the pre-ACoA aneurysm formation model was 7 553 mm^3, the volume of the pre-ICA aneurysm growth model-2 was 4 014 mm^3, and the volume of the pre-ICA aneurysm growth model-1 was 1 718 mm^3.

Wall shear stress distribution in the aneurysm models

In each of the four models, there was high wall shear stress in the region of flow impingement of the internal carotid artery aneurysm, and low wall shear stress in the remainder of the internal carotid artery aneurysm (Figure 2). With increasing size of the aneurysm, the area of low wall shear stress increased. The whole

aneurysm and an anterior communicating artery aneurysm had very low wall shear stress. The wall shear stress of the aneurysm and an anterior communicating artery was lower than that of the anterior cerebral artery, internal carotid artery, and middle cerebral artery.

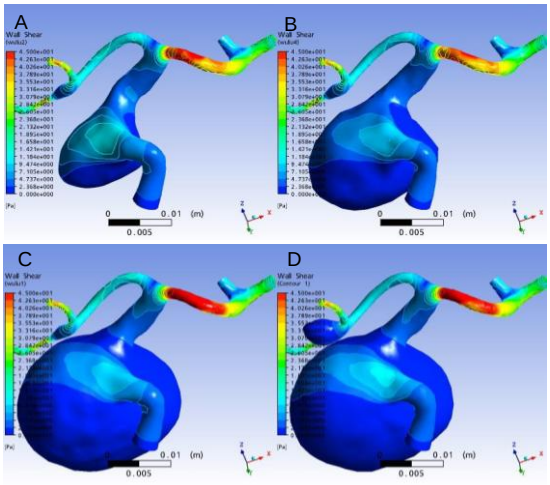

Figure 2 Contour images of the wall shear stress distributions in the four aneurysm models.

As the internal carotid artery (ICA) aneurysm enlarged, the area of low wall shear stress increased. (A) Pre-ICA aneurysm growth model-1. (B) Pre-ICA aneurysm growth model-2. (C) Pre-anterior communicating artery (ACoA) aneurysm formation model. (D) Post-ACoA aneurysm formation model. The red represents high wall shear stress and the blue represents low wall shear stress.

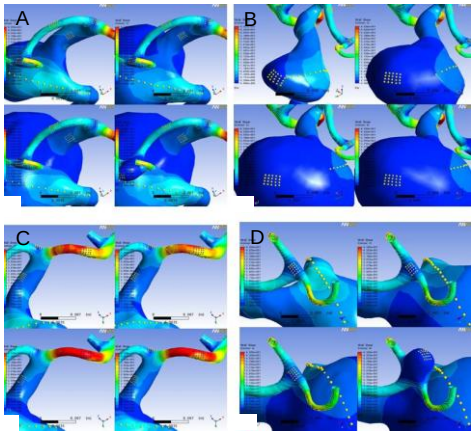

Figure 3 Wall shear stress (WSS) in selected regions of the aneurysms and the surrounding arteries in the four aneurysm models.

Twenty yellow points were selected at each of the anterior communicating artery (ACoA), ACoA aneurysm, anterior cerebral artery (ACA), internal carotid artery (ICA), middle cerebral artery (MCA), bifurcation of the ICA, bifurcation of the MCA, inflow region of the ICA aneurysm, and dome of the ICA aneurysm. The red represents high WSS and the blue represents low WSS.

(A) The inflow region of the ICA aneurysm, bifurcation of the ICA, ICA, and ACA. (B) The dome of the ICA aneurysm. (C) The MCA. (D) The ACoA and ACoA aneurysm.

In each figure part, the left upper model is the pre-ICA aneurysm growth model-1, the right upper model is the pre-ICA aneurysm growth model-2, the left lower model is the pre-ACoA aneurysm formation model, and the right lower model is the post-ACoA aneurysm formation model.

Wall shear stress changes in various regions of the aneurysms and surrounding arteries in the aneurysm models

We selected some specific points on the aneurysms to compare wall shear stress among the four models (Figure 3). As aneurysms often originate at the bifurcations of arteries, we selected points in the aneurysm and an anterior communicating artery and at the bifurcations of the internal carotid artery and middle cerebral artery to calculate wall shear stress. As aneurysms most frequently rupture at the dome, we also selected points on the domes of the aneurysms in each of the four models. In the wall of the internal carotid artery aneurysm, the wall shear stress was high in the region of flow impingement and decreased at the inflow region. We also selected 20 points along the path of blood flow in the middle parts of the anterior cerebral artery and middle cerebral artery and the distal part of the internal carotid artery to examine wall shear stress in healthy arteries (Figure 3). The transient wall shear stress at peak-systole (0.31 second) was calculated at the selected points.

Wall shear stress curves of different aneurysm models

For each model, the wall shear stress at peak-systole (0.31 second) of each of the 20 points in each region was calculated. The wall shear stress at the dome of the internal carotid artery aneurysm decreased with increasing size of the aneurysm (Figure 4A). There were no significant differences in wall shear stress at the inflow region of the internal carotid artery aneurysm among the four models (Figure 4B). The wall shear stress of the aneurysm and an anterior communicating artery was low in the internal carotid artery aneurysm growth models, and was not significantly different among the four models. The wall shear stress of the aneurysm and an anterior communicating artery aneurysm was very low on the post-aneurysm and an anterior communicating artery aneurysm model compared with the other three models (Figure 4C). The wall shear stress of the aneurysm and an anterior communicating artery was lower than that at the bifurcations of the middle cerebral artery and internal carotid artery in the pre-aneurysm and an anterior communicating artery aneurysm formation models (Figure 4D).

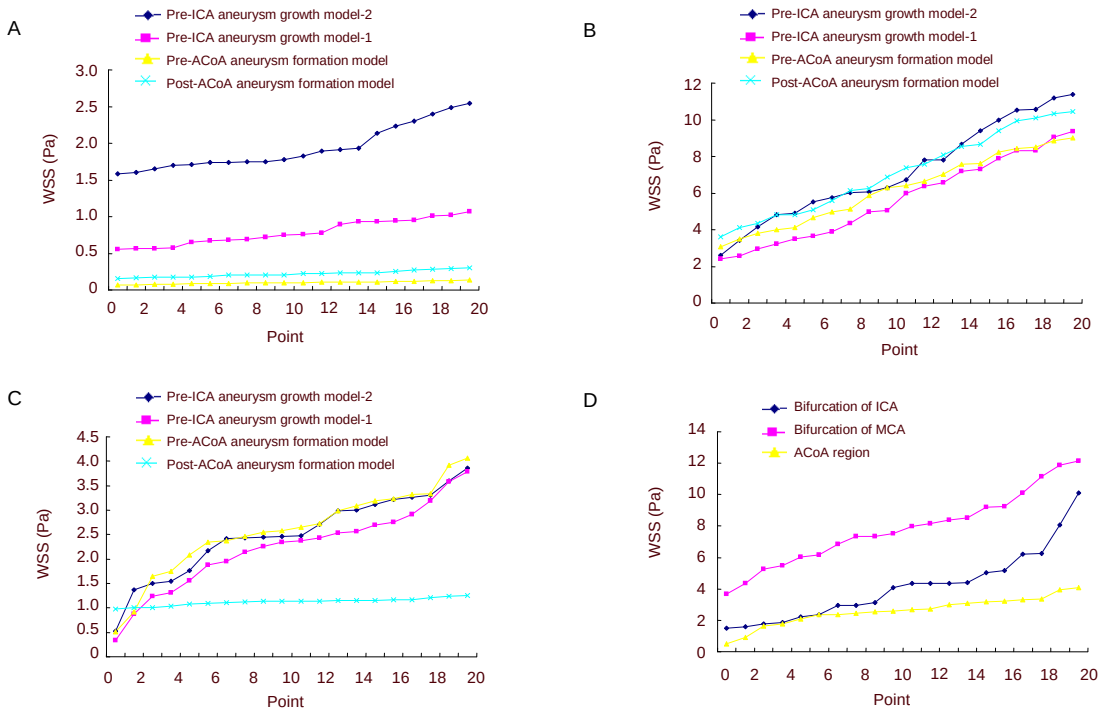

Figure 4 Comparison of wall shear stress (WSS) among the different aneurysm models.

(A) WSS at 20 points on the dome of the internal carotid artery (ICA) aneurysm in each of the four models. (B) WSS at 20 points along the inflow region of the ICA aneurysm in each of the four models. (C) WSS at 20 points along the anterior communicating artery (ACoA) and at the ACoA aneurysm in each of the four models. (D) WSS at 20 points along the ACoA, at the bifurcation of the middle cerebral artery (MCA), and at the bifurcation of the ICA in the pre-ACoA aneurysm formation model. (A–D) The X-axis shows 20 points presented in increasing magnitude of WSS.

Statistical analysis of the wall shear stress data

Data were analyzed according to a growth model (comparing the pre-internal carotid artery aneurysm growth model-1 with model-2) and a formation model (comparing the pre-aneurysm and an anterior communicating artery aneurysm formation model with the post-aneurysm and an anterior communicating artery aneurysm formation model; Table 1). In the growth model, the wall shear stress at the dome of the internal carotid artery aneurysm decreased significantly when the internal carotid artery aneurysm increased in size (P < 0.01). In the formation model, the wall shear stress at the dome of the internal carotid artery aneurysm increased significantly after formation of aneurysm and an anterior communicating artery aneurysm (P < 0.01). In the growth model, the wall shear stress at the inflow region of the internal carotid artery aneurysm did not change significantly when the internal carotid artery aneurysm increased in size (P = 0.114 5). In the formation model, the wall shear stress at the inflow region of the internal carotid artery aneurysm did not change significantly after formation of the aneurysm and an anterior communicating artery aneurysm (P = 0.176 5). In the growth model, the wall shear stress of the aneurysm and an anterior communicating artery did not change significantly when the internal carotid artery aneurysm increased in size (P = 0.412 4). In the formation model, the wall shear stress of the aneurysm and an anterior communicating artery decreased significantly after formation of the aneurysm and an anterior communicating artery aneurysm (P < 0.01). In the growth model, the wall shear stress at the internal carotid artery bifurcation did not change significantly when the internal carotid artery aneurysm increased in size (P = 0.502 0). In the formation model, the wall shear stress at the internal carotid artery bifurcation did not change significantly after formation of the aneurysm and an anterior communicating artery aneurysm (P = 0.718 3). In the growth model, the wall shear stress at the middle cerebral artery bifurcation changed significantly when the internal carotid artery aneurysm increased in size (P < 0.01). In the formation model, the wall shear stress at the middle cerebral artery bifurcation did not change significantly after formation of the aneurysm and an anterior communicating artery aneurysm (P = 0.144 4). In the growth model, the wall shear stress of the distal part of the internal carotid artery changed significantly when the internal carotid artery aneurysm increased in size (P < 0.01).

Table 1 Average wall shear stress in different locations

Location	Pre-ICA aneurysm growth model-2	Pre-ICA aneurysm growth model-1	Pre-ACoA aneurysm formation model	Post-ACoA aneurysm formation model	Growth model		Formation model	
					F	*P*	*F*	*P*
ICA aneurysms dome	1.93±0.30	0.78±0.17	0.10±0.02	0.22±0.04	425.76	< 0.01	130.13	< 0.01
ICA aneurysm inflow area	7.17±2.67	5.64±2.28	6.19±1.94	7.11±2.26	2.25	> 0.05	1.90	> 0.05
ACoA region	2.51±0.84	2.24±0.87	2.59±0.90	1.12±0.08	0.90	> 0.05	52.75	< 0.01
ICA bifurcation	4.10±2.29	3.43±1.90	4.13±2.26	3.87±2.32	0.70	> 0.05	0.13	> 0.05
MCA bifurcation	9.24±1.81	6.11±2.20	7.84±2.35	8.88±2.08	10.84	< 0.01	2.22	0.14
Distal part of the ICA	4.63±0.08	4.37±0.13	4.55±0.13	4.66±0.12	26.31	< 0.01	7.81	< 0.01
Middle part of MCA	37.73±2.57	36.87±2.08	49.75±3.64	41.23±2.43	128.90	< 0.01	76.14	< 0.01
Middle part of ACA	12.30±0.24	11.38±0.14	12.28±0.26	11.61±0.16	113.93	< 0.01	94.00	< 0.01

Measurement data are presented as mean ± SD, n = 20. One-way analysis of variance was used to analyze the differences between the models in each region. ICA: Internal carotid artery; ACoA: anterior communicating artery; MCA: middle cerebral artery; ACA: anterior cerebral artery.

In the formation model, the wall shear stress of the distal part of the internal carotid artery increased significantly after formation of the aneurysm and an anterior communicating artery aneurysm (P < 0.01). In the growth model, the wall shear stress of the middle part of the middle cerebral artery changed significantly when the internal carotid artery aneurysm increased in size (P < 0.01). In the formation model, the wall shear stress of the middle part of the middle cerebral artery decreased significantly after formation of the aneurysm and an anterior communicating artery aneurysm (P < 0.01).In the growth model, the wall shear stress of the middle part of the anterior cerebral artery changed significantly when the internal carotid artery aneurysm increased in size (P < 0.01). In the formation model, the wall shear stress of the middle part of the anterior cerebral artery decreased significantly after formation of the aneurysm and an anterior communicating artery aneurysm (P < 0.01).

DISCUSSION

Flow dynamics play an important role in the initiation, growth, and rupture of cerebral artery aneurysms. Wall shear stress is a flow-induced stress that can be described as the frictional force of viscous blood. Some researchers have conducted studies of hemodynamic parameters using data from follow-up angiography examinations. Jou *et al* [4] conducted a 2-year follow-up study of two patients with basilar fusiform aneurysms of a similar size. In the aneurysm that grew in size, the area of low wall shear stress (< 0.1 N/m^2) increased from 270 mm^2 to 430 mm^2. The general flow patterns did not change over time in either of the aneurysms, but the wall shear stress histograms were very different in these two patients. Tateshimaa *et al* [5] followed a growing middle cerebral artery aneurysm with a bleb over 1 year, and reported that the longest diameter of the dome of the middle cerebral artery aneurysm increased from 4 mm to 6 mm, and that the wall shear stress within the bleb remained low throughout this period. Boussel *et al* [7] followed seven patients with intracranial arterial aneurysms that were unsuitable for direct surgical treatment with MRI studies every 6 to 12 months. Their findings indicated that aneurysm growth was likely to occur in regions exposed to abnormally low wall shear stress, and that the hemodynamic parameters changed as the aneurysms enlarged. However, all the above studies had some limitations. It is difficult to study changes in hemodynamic parameters during aneurysm formation or growth. As increasing aneurysm size increases the risk of rupture, it is very important to assess the flow dynamics of growing aneurysms.

In this study, we reconstructed the geometry of an internal carotid artery aneurysm to simulate it at various stages of growth. The volume of the internal carotid artery aneurysm decreased by 3 539 mm^3 in the pre-aneurysm and an anterior communicating artery aneurysm formation model-2, and by a further 2 296 mm^3 in model-1. Some researchers have tried to reconstruct the original geometry of the vessels by removing the aneurysm. Tremmel *et al* [8] found that the aneurysm luminal area that was exposed to low wall shear stress increased with increasing aneurysm-to-parent vessel size ratios. Although there was a relationship between the aneurysm-to-parent vessel size ratio and the hemodynamic parameters within aneurysms, they found that the geometry and size of the parent arteries and aneurysms were more strongly associated with wall shear stress than the size ratio. In our study using MIMICS software, we were able to achieve good reconstructions of the aneurysms and neighboring arteries. Using the remesh module, areas that needed to be decreased in size were selected, and the parameters for

change were determined so that the shape and size of the aneurysms could be changed while keeping all other morphological parameters constant. In these models, the structures of the upstream and downstream arteries were maintained, so that the influence of the growing aneurysms on the hemodynamic parameters within the aneurysms and in the adjacent arteries could be evaluated.

The size and tapering of the internal carotid artery may influence the wall shear stress, with higher wall shear for smaller arteries and lower wall shear for larger arteries. Aneurysm size influences the wall shear stress of the aneurysm. The wall shear stress was reported to be high in the region where the blood entered the aneurysm, and relatively low in the remainder of the aneurysm[9]. In the larger aneurysm model, there were more vortices within the aneurysm, and more areas of low velocity blood flow were detected. Our data showed that the three aneurysm growth models had larger areas of low wall shear stress than the post-aneurysm and an anterior communicating artery model, and that the area of low wall shear stress increased as aneurysm size increased. The wall shear stress at the dome of the aneurysm decreased significantly with increasing aneurysm size, but the wall shear stress at the neck and inflow region of the aneurysm did not change significantly with increasing aneurysm size.

Wall shear stress is a dynamic frictional force induced by a viscous fluid moving along a solid surface. The endothelium regulates local vascular tone by releasing vasodilator and vasoconstrictor substances. Wall shear stress has a stronger influence on blood vessels *via* its effects on various endothelial functions than *via* direct mechanical forces[10-11]. Chronic low wall shear stress may alter the expression of biological markers of vascular remodeling[12]. Low wall shear stress can also trigger apoptosis of endothelial cells resulting in vessel wall degeneration[13]. It seems reasonable to assume that low wall shear stress results in a loss of mechanical resistance of the vessel wall, which may contribute to the growth of aneurysms.

It has been reported that high wall shear stress might stimulate the production of matrix metalloproteinases by endothelial cells, which are likely to be instigators of internal elastic lamina degradation of the arterial wall[14]. Destructive remodeling of the extracellular matrix has been shown in the aneurysmal abdominal aorta[15-16]. It has been postulated in animal studies that focal high wall shear stress rather than focal mechanical stress predisposes to aneurysm formation in healthy cerebral arteries[17-18]. High wall shear stress may therefore also contribute to aneurysm formation. However, our results did not show that high wall shear stress was associated with aneurysm development. Blood vessels are also exposed to other forces induced by pulsatile blood flow such as hydrostatic and dynamic pressure. The hydrostatic pressure is nearly equivalent to the blood pressure. Dynamic pressure is the force produced by impingement of the blood flow on the arterial wall, and is superimposed on the hydrostatic pressure. However, the dynamic pressure is very small compared with normal blood pressure, and may not be a significant factor in the growth aneurysms. Aneurysm geometry is influenced by the flow and wall shear stress within the aneurysm, and also by the geometry of the parent vessel, which contributes to the hemodynamic parameters within the aneurysm[19-20]. However, it remains poorly understood whether the morphology of the growing aneurysm affects the parent vessel and adjacent arteries. In this study, we found that the wall shear stress of the parent arteries changed significantly as the internal carotid artery aneurysm increased in size, except in the aneurysm and an anterior communicating artery artery and at the internal carotid artery bifurcation. The wall shear stress of the aneurysm and an anterior communicating artery was consistently low in the three aneurysm growth models, with no significant differences among the three models. The wall shear stress of the aneurysm and an anterior communicating artery was significantly lower than the wall shear stress at the bifurcations of the internal carotid artery and middle cerebral artery in all three models, which may correlate with the local origin of the aneurysm. Doenitz *et al* [21] reported a patient with *de novo* formation of a basilar artery aneurysm and subsequent rupture within 44 days. They proposed a potential mechanism for the formation of this aneurysm. Based on the assumption of preexisting reduced resistance of the vessel wall to pressure changes and an area of permanently low wall shear stress, increased intravascular pressure could have induced geometrical changes, with subsequent changes in the intravascular flow distribution, thereby further lowering the wall shear stress in specific locations, leading to endothelial damage with decreased stability of the vessel wall and aneurysm development.

In some cases, an increasing portion of the wall of the parent artery adjacent to the aneurysm becomes incorporated into the wall of the aneurysm. Hemodynamic changes in the adjacent vessels during growth of the aneurysm may contribute to this process.

An aneurysm may recur or rupture after endovascular coiling (because of coil compaction) or after surgical clipping (because of aneurysm remnants, which may be partially due to pathological factors such as congenital defects, hypertension, or atherosclerosis). Hemodynamic changes may also play an important role in the post-treatment pathogenesis of aneurysms. Ortega *et al* [22] performed computational fluid dynamic simulations of the basilar artery aneurysm and bifurcation of a patient before and after virtual endovascular treatment. The study demonstrated that it was possible for successful isolation of the aneurysm from the circulation, leaving no aneurysm neck remnant, to result in increased hemodynamic stresses that could injure the arterial wall. There are no previous reports describing the impact of new aneurysm formation on the hemodynamic parameters within a preexisting aneurysm. We studied a model of a patient with one larger and one smaller aneurysm. We assumed that the larger aneurysm formed first, and that formation of the second aneurysm may have caused hemodynamic changes within the first aneurysm and in the upstream artery. We found that the wall shear stress at the dome of the internal carotid artery aneurysm increased significantly from 0.099 ± 0.019 Pa to 0.219 ± 0.043 Pa after formation of the aneurysm and an anterior communicating artery aneurysm, but that the hemodynamic parameters at the neck and inflow region of the internal carotid artery aneurysm remained unchanged. After formation of the aneurysm and an anterior communicating artery aneurysm, the wall shear stress decreased significantly in the anterior cerebral artery and middle cerebral artery and increased significantly in the distal part of the internal carotid artery, but did not change significantly at the bifurcations of the internal carotid artery and middle cerebral artery. The hemodynamic parameters of the first aneurysm changed after formation of the second aneurysm, as the blood flow became more complex in the aneurysms and adjacent arteries. Further research should be conducted to elucidate these changes.

In this study, we used data from a patient with two aneurysms to construct four models that simulated different stages of aneurysm formation and growth. We found that the area of low wall shear stress increased, and the wall shear stress decreased, with increasing size of the internal carotid artery aneurysm. In the pre-aneurysm and an anterior communicating artery aneurysm formation model, we found that the wall shear stress was low at the location of aneurysm formation in the aneurysm and an anterior communicating artery. The hemodynamic parameters in the adjacent arteries changed significantly during the stages of aneurysm formation and growth.

SUBJECTS AND METHODS

Design

Digital medicine and imaging study.

Time and setting

The experiments were performed in the laboratory of the Department of Neurosurgery of Chinese PLA General Hospital, China from May 2011 to February 2012.

Subjects

A 58-year-old woman presented with 1-year history of impaired vision. CT angiography showed two intracranial aneurysms, which were both clipped during a single procedure. The patient provided informed consent before the procedure.

Methods

CT angiography

CT angiography[23] was performed using a multidetector-row helical CT scanner (LightSpeed 16, General Electric Healthcare Corporation, Waukesha, WI, USA; Figure 5).

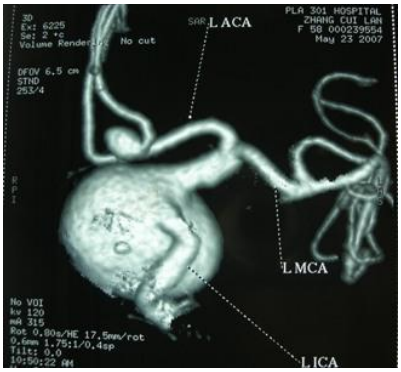

Figure 5 CT angiography of the patient used to construct the model, showing a large internal carotid artery paraclinoid aneurysm and a small anterior communicating artery aneurysm.

L-ACA: Left anterior cerebral artery; L-MCA: left middle cerebral artery; L-ICA: left internal carotid artery.

The slice thickness was 0.625 mm and table speed was 9 mm/s (120 kV, 315 mAs). DICOM format sections were reconstructed in a 512 × 512 matrix.

Construction of aneurysm models

Using MIMICS 10.0 software (Belgium Materialise

Company), we defined the region of interest and extracted the luminal vascular surface from the 3D raster gray-scale image to construct the post-aneurysm and an anterior communicating artery aneurysm formation model. We constructed a pre-aneurysm and an anterior communicating artery aneurysm formation model by removing the aneurysm and an anterior communicating artery aneurysm, and then further constructed a pre-internal carotid artery aneurysm growth model-2 (by decreasing the size of the internal carotid artery aneurysm) and a pre-internal carotid artery aneurysm growth model-1 (by further decreasing the size of the internal carotid artery aneurysm). These models were obtained using the remesh module of the MIMICS interactive image control software. The areas that needed to be decreased in size were selected, the smooth function was used, and parameters were set to control the changes. The shape and size of the aneurysms could then be constructed as required (Figure 1). The pre-aneurysm and an anterior communicating artery aneurysm formation model was considered to represent the stage immediately preceding the initiation of aneurysm and an anterior communicating artery aneurysm formation. The models with decreased internal carotid artery aneurysm size represented the stages of internal carotid artery aneurysm growth. Workbench 11.0 software (ANSYS Inc., Canonsburg, PA, USA) was used to divide the fluid model into tetrahedral cells. Mesh independence was performed to determine the optimum number of elements.

Numerical methods

As previously described[23], for the fluid domain, the blood flow was assumed to be laminar and Newtonian. Incompressible Navier-Stokes equations, which are suitable for analysis of models with fluid-solid interactions, were used as the governing equations. Numerical modeling was performed using commercially available ANSYS-CFX11 software (ANSYS Inc., Canonsburg, PA, USA). The inlet boundary condition was set by specifying a velocity pulse at the inlet for a period of 1 second. The density of the blood was set at 1 050 kg/m^3. Structural analysis was performed using the commercially available ANSYS- Mechanical software (ANSYS). The governing equation for the structural domain was the momentum conservation equation. The artery wall was assumed to be elastic, isotropic, incompressible, and homogeneous with a density of 1 050 kg/m^3 and a Poisson's ratio of 0.45. Three cardiac cycles with 100 time-steps per cycle were computed, and all data used corresponded to the third cardiac cycle.

Statistical analysis

Measurements were presented as mean ± SD. One-way analysis of variance was used to analyze the differences in each region among the models. All statistical analyses were performed using SPSS 12.0 software (SPSS, Chicago, IL, USA). For each model, the wall shear stress was recorded during peak-systole (0.31 second) at 20 points in each of the locations studied. The mean wall shear stress during peak-systole was then calculated for each region. Differences were considered statistically significant at $P < 0.01$.

Acknowledgments: We thank Haiyu Ju, Department of Radiology, Chinese PLA General Hospital, for analysis of the CT angiography data.

Funding: This work was supported by the National Natural Science Foundation of China, No. 81171109.

Author contributions: Fuyu Wang and Bainan Xu defined the research theme. Fuyu Wang, Bainan Xu, and Zhenghui Sun designed the experiments, analyzed the data, interpreted the results, and wrote the paper. Chen Wu worked on the collection and interpretation of associated data. Xiaojun Zhang co-designed the experiments, and discussed the analyses, interpretations, and presentation. All authors contributed to, read, and approved the manuscript.

Conflicts of interest: None declared.

Ethical approval: The study was approved by the Ethics Committee of Chinese PLA General Hospital.

Author statements: The manuscript is original, has not been submitted to any other publication, and has not been previously published in any language or any form, including electronic. The manuscript contains no disclosure of confidential information or authorship/patent application/funding source disputations.

REFERENCES

[1] Satoh T, Onoda K, Tsuchimoto S. Visualization of intraaneurysmal flow patterns with transluminal flow images of 3D MR angiograms in conjunction with aneurysmal configurations. AJNR Am J Neuroradiol. 2003;24(7):1436-1445.

[2] Tateshima S, Murayama Y, Villablanca JP, et al. In vitro measurement of fluid-induced wall shear stress in unruptured cerebral aneurysms harboring blebs. Stroke. 2003;34(1):187-192.

[3] Asari S, Ohmoto T. Natural history and risk factors of unruptured cerebral aneurysms. Clin Neurol Neurosurg. 1993;95(3):205-214.

[4] Jou LD, Wong G, Dispensa B, et al. Correlation between lumenal geometry changes and hemodynamics in fusiform intracranial aneurysms. AJNR Am J Neuroradiol. 2005;26(9):2357-2363.

[5] Tateshimaa S, Tanishitab K, Omurab H, et al. Intra-aneurysmal hemodynamics during the growth of an unruptured aneurysm: in vitro study using longitudinal CT angiogram database. AJNR Am J Neuroradiol. 2007;28(4): 622-627.
[6] Mantha A, Karmonik C, Benndorf G, et al. Hemodynamics in a cerebral artery before and after the formation of an aneurysm. AJNR Am J Neuroradiol. 2006;27(5): 1113-1118.
[7] Boussel L, Rayz V, McCulloch C, et al. Aneurysm growth occurs at region of low wall shear stress, patient-specific correlation of hemodynamics and growth in a longitudinal study. Stroke. 2008;39(11):2997-3002.
[8] Tremmel M, Dhar S, Levy EI, et al. Influence of intracranial aneurysm-to-parent vessel size ratio on hemodynamics and implication for rupture: results from a virtual experimental study. Neurosurgery. 2009;64(4): 622-631.
[9] Jou LD, Lee DH, Morsi H, et al. Wall shear stress on ruptured and unruptured intracranial aneurysms at the internal carotid artery. AJNR Am J Neuroradiol. 2008; 29(9):1761-1767.
[10] Luscher TF, Tanner FC. Endothelial regulation of vascular tone and growth. Am J Hypertens. 1993;6(7):283S-293S.
[11] Stamler JS. Redox signaling: nitrosylation and related target interactions of nitrous oxide. Cell. 1994;78(6): 931-936.
[12] Kadirvel R, Ding YH, Dai D, et al. The influence of hemodynamic forces on biomarkers in the walls of elastase-induced aneurysms in rabbits. Neuroradiology. 2007;49(12):1041-1053.
[13] Kaiser D, Freyberg MA, Friedl P. Lack of hemodynamic forces triggers apoptosis in vascular endothelial cells. Biochem Biophys Res Commun. 1997;231(3):586-590.
[14] Sho E, Sho M, Singh TM, et al. Arterial enlargement in response to high flow requires early expression of matrix metalloproteinases to degrade extracellular matrix. Exp Mol Pathol. 2002;73(2):142-153.
[15] Tromp G, Gatalica Z, Skunca M, et al. Elevated expression of matrix metalloproteinase-13 in abdominal aortic aneurysms. Ann Vasc Surg. 2004;18(4):414-420.
[16] Kataoka K, Taneda M, Asai T, et al. Structural fragility and inflammatory response of ruptured cerebral aneurysms: a comparative study between ruptured and unruptured cerebral aneurysms. Stroke. 1999;30(7):1396-1401.
[17] Fukuda S, Hashimoto N, Naritomi H, et al. Prevention of rat cerebral aneurysm formation by inhibition of nitric oxide synthase. Circulation. 2000;101(21):2532-2538.
[18] Sadamasa N, Nozaki K, Hashimoto N. Disruption of gene for inducible nitric oxide synthase reduces progression of cerebral aneurysms. Stroke. 2003;34(12):2980-2984.
[19] Hassan T, Timofeev EV, Saito T, et al. A proposed parent vessel geometry-based categorization of saccular intracranial aneurysms: Computational flow dynamics analysis of the risk factors for lesion rupture. J Neurosurg. 2005;103(6):662-680.
[20] Hoi Y, Meng H, Woodward SH, et al. Effects of arterial geometry on aneurysm growth: Three-dimensional computational fluid dynamics study. J Neurosurg. 2004; 101(4):676-681.
[21] Doenitz C, Schebesch KM, Zoephel R, et al. A mechanism for the rapid development of intracranial aneurysms: a case study. Neurosurgery. 2010;67(5):1213-1221.
[22] Ortega J, Hartman J, Rodriguez J, et al. Post-treatment hemodynamics of a basilar aneurysm and bifurcation. Ann Biomed Eng. 2008;36(9):1531-1546.
[23] Xu BN, Wang FY, Liu L, et al. Hemodynamics model of fluid-solid interaction in internal carotid artery aneurysms. Neurosurg Rev. 2011;34(1):39-47.

(Reviewed by Elgin M, Raye W, Wang MD, Wang YJ)
(Edited by Wang J, Su LL, Li CH, Song LP)